Carrier distribution in InGaN/GaN tricolor multiple quantum well light emitting diodes

R. Charash' , P. P. Maaskant, L. Lewis, C. McAleese, M. J. Kappers, C. J. Humphreys, and B. Corbett

Citation: Appl. Phys. Lett. **95**, 151103 (2009); doi: 10.1063/1.3244203
View online: http://dx.doi.org/10.1063/1.3244203
View Table of Contents: http://aip.scitation.org/toc/apl/95/15
Published by the American Institute of Physics

Carrier distribution in InGaN/GaN tricolor multiple quantum well light emitting diodes

R. Charash,[1,a)] P. P. Maaskant,[1] L. Lewis,[1] C. McAleese,[2] M. J. Kappers,[2] C. J. Humphreys,[2] and B. Corbett[1]
[1]*Tyndall National Institute, University College Cork, Lee Maltings, Cork, Ireland*
[2]*Department of Materials Science and Metallurgy, University of Cambridge, Pembroke Street, Cambridge CB2 3QZ, United Kingdom*

(Received 12 July 2009; accepted 4 September 2009; published online 12 October 2009)

Carrier transport in InGaN light emitting diodes has been studied by comparing the electroluminescence (EL) from a set of triple quantum well structures with different indium content in each well, leading to multicolor emission. Both the sequence and width of the quantum wells have been varied. Comparison of the EL spectra reveals the current dependent carrier transport between the quantum wells, with a net carrier flow toward the deepest quantum well. © *2009 American Institute of Physics*. [doi:10.1063/1.3244203]

Solid state lighting applications require light emitting diodes (LEDs) based on III-nitride semiconductors with high internal quantum efficiencies at high current densities. High current densities lead to high carrier densities in the active region, and consequently a significant amount of nonradiative Auger recombination.[1] An increase in the internal quantum efficiency at higher current densities can be achieved by spreading the carriers over a larger volume, either through the employment of a double heterostructure or by using a multiquantum well (MQW) active region.[2] In a MQW configuration, it is important to have a uniform distribution of carriers across all the quantum wells. Experimental information about carrier distributions can be obtained from quantum well structures with different indium content in each of the InGaN quantum wells: each well then emits its own characteristic color.[3–7] In this way one can also monitor how a carrier distribution evolves with increasing bias current. The factors that determine the carrier transport between quantum wells are the effective mass of the carriers, and the height and thickness of the barriers, both in the conduction band and in the valence band. In situations where all quantum wells are identical, the relatively large effective mass of the holes, as compared to the effective mass of the electrons, tends to make hole transport the limiting factor in achieving a uniform carrier distribution.[8] The effect of barrier thickness on carrier distribution has also been studied in InGaAsP lasers where a large valence band offset is present.[9] Apart from their use in monitoring carrier distributions, multicolor LEDs are also useful as broad-spectrum LED sources.

In this letter, we compare the emission characteristics from four LED structures, each containing three InGaN quantum wells with different amounts of indium in individual wells. The thickness of the wells and the sequence of the wells are varied in order to help identify those contributing to the light emission. We show that the emission depends on both the position and confinement (depth) of the quantum wells, with one or two wells dominating in most cases. A superlinear light output characteristic is measured in one sample.

The LED structures were grown by metal-organic vapor phase epitaxy on sapphire substrates where the GaN buffer layer had an estimated dislocation density of $\sim 5 \times 10^9$ cm^{-2}. Following the growth of an *n*-GaN layer, three InGaN quantum wells with 6 nm thick GaN barriers were grown with differing indium content in each well. A 130 nm thick Mg-doped *p*-GaN layer completed the structures. In all cases, the *p*-GaN was grown at 925 °C to prevent thermal decomposition of the wells. Two of the samples (A and B) were grown with narrow quantum wells (1.2–2 nm) while two other samples (C and D) had broader wells (2–3 nm). This results in different confinement energies for electrons and holes in each well. Samples A and D were with a shallow well adjacent to the *p* side, a deep well (highest indium content) adjacent to the *n* side and an intermediate indium content well between these two. The order of the quantum wells was reversed in samples B and C. Figure 1 shows the schematic of the four structures and Table I shows the detailed well configurations. Room temperature photoluminescence (PL) measurements of the LED structures confirmed the presence of the separate quantum well layers.

LEDs were fabricated by depositing 50 μm diameter Pd/Pt/Au (3/5/500 nm) *p*-type contacts by electron beam

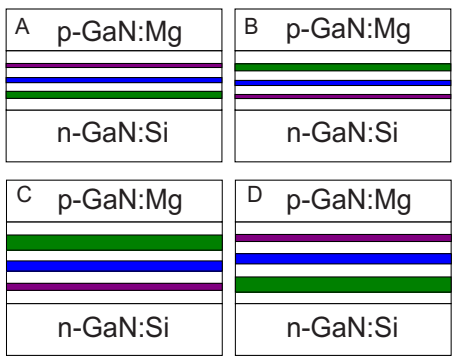

FIG. 1. (Color online) Schematic representation of the four InGaN/GaN MQW LED layer structures. Structures A and B use narrow quantum wells with the shallow and deep well adjacent to the *p* side, respectively, C and D use wider quantum wells with the deep and shallow well adjacent to the *p* side, respectively.

a)Electronic mail: ragh.charash@tyndall.ie.

TABLE I. Details of the well configurations from the four LED structures. QW-1 refers to the quantum well closest to the *n* side.

	Indium content (%)			Well widths (nm)			Nominal emission wavelength (nm)		
Sample	QW-3	QW-2	QW-1	QW-3	QW-2	QW-1	QW-3	QW-2	QW-1
A	5	15	25	1.2	1.6	2.0	380	430	490
B	25	15	5	2.0	1.6	1.2	490	430	380
C	25	15	5	3.0	2.5	2.0	560	460	400
D	5	15	25	2.0	2.5	3.0	400	460	560

evaporation and lift off. The contacts were evaluated by circular transmission line measurements. The contacts on all samples produced linear current-voltage (*I-V*) characteristics, indicating that the contacts are ohmic. The extracted *p*-GaN resistivity values on the different samples lay in the range of 1.6–2.4 Ω cm and the specific contact resistivity values in the range of 10^{-3}–10^{-2} Ω cm^2. The *p* contacts were isolated from each other by mesa-etching down to the *n*-GaN layer, using reactive ion etching with the *p* metal as a mask. The metallized border of the wafer pieces was used as an *n* contact.

The devices were characterized at room temperature under swept current-voltage (*I-V*) conditions. Figure 2 shows the forward log *I-V* characteristics of typical devices from A, B, C, and D. The diode ideality factors are lower for the devices with the narrow quantum wells (A and B). The ideality factor is linked to the efficiency of the electron-hole recombination process, and indeed, we observe higher light outputs on samples A and B, i.e., the samples with the lower ideality factors [Fig. 3(a)]. It is noted that the voltage at which the ideality reaches its minimum ($I \sim 1$ μA) is ~250 mV lower for sample B in comparison with sample A, despite the only difference between the samples being the order of the quantum wells. Later we show that this voltage differential corresponds to the difference in the dominant emission energy, confirming that this current is due to radiative recombination through the dominant quantum well. Thus, the *p-n* junction is located toward the *p* side of the quantum well region. Samples C and D show higher leakage currents, indicative of more nonradiative recombination. We attribute the extra leakage current to defects associated with the higher strain, resulting from the thicker quantum wells.

Figure 3 shows the *L-I* characteristics from the different LEDs at room temperature. The light intensity was measured through the transparent substrate with a silicon photodiode of numerical aperture 0.5. The light output from the samples with narrow quantum wells was higher than from the samples with wider quantum wells, due to the quantum confined Stark effect, which results in poorer electron-hole overlap in the thicker quantum wells.[10] This is due to the larger separation between the electrons and holes in the wider quantum wells in the presence of the piezoelectric field, resulting in longer radiative recombination times.[11] It is noted that samples A, B, and D show a droop in the *L-I* curve at high current densities, whereas sample C, which is the least efficient device at low current densities, shows a super linear increase in the light output up to current densities of 5 kA/cm^2.

Figure 4 shows the normalized room temperature electroluminescence (EL) spectra from the four samples, at current densities of ~500 A/cm^2 and ~2500 A/cm^2. Note that these current densities are beyond the values found in most commercial LED devices. To obtain the EL spectra, the light was collected through the top surface into a fiber coupled spectrometer. The angle between the fiber and the surface normal was 60°.

To interpret the observed spectra we propose the following model, illustrated in Fig. 5 (for sample A only).[12] The model is based on the following assumptions: (1) The amount of carriers captured per well decreases as carriers penetrate deeper into the quantum well structure. (2) Once captured, the carriers quickly relax toward the bottom of the wells. (3) Due to the quick relaxation of captured carriers, the net transport of carriers between quantum wells (both through tunnelling and through thermionic emission) is in the direction of the deepest quantum well.

Sample A shows two emission peaks in the EL (Fig. 4), the emission from the third quantum well adjacent to the *p* side is missing (please note the wells are numbered according to their growth order). This must be due to a lack of electrons in this quantum well as holes will readily reach this well. In the PL (not shown) all three quantum wells are evi-

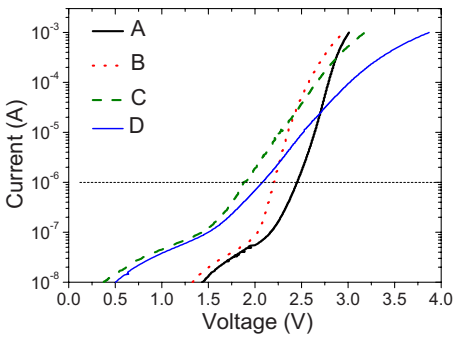

FIG. 2. (Color online) *I-V* curves from InGaN/GaN LEDs A, B, C, and D. The dashed line indicates a current of 1 μA.

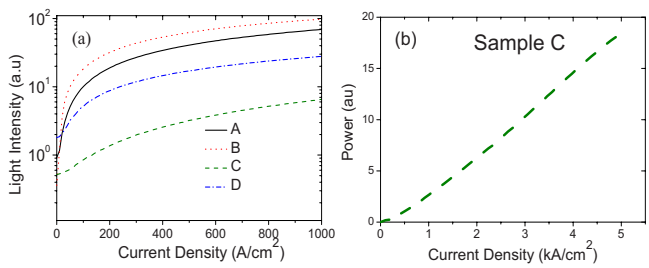

FIG. 3. (Color online) (a) *L-I* curves on a logarithmic scale. (b) shows the *L-I* characteristic of sample C on a linear scale up to 5 kA/cm^2.

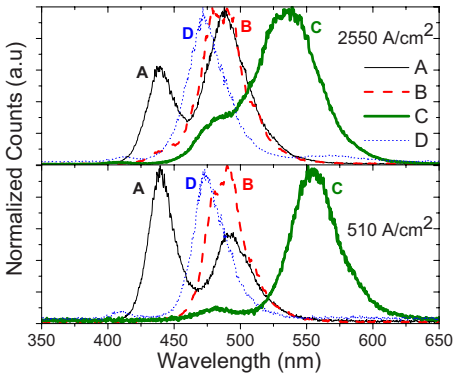

FIG. 4. (Color online) Normalized EL spectra comparing the emission from different LED structures A, B, C, and D at two current densities (510 and 2550 A/cm^2).

dent. The fact that holes populate all quantum wells, while electrons are failing to reach the third quantum well, agrees with the assumption that in this structure there is significant hole transport between the wells, and that this transport is directed toward the deepest well (in this case, well 1).

Sample B is the sample with the highest light output. At low bias, only the emission from the deepest well (well 3) is visible, while at high bias there is a faint signature from well 2 also. Given that electrons are able to reach the well that is furthest from the *n* side, we can assume that electrons populate all three quantum wells, and that the lack of emission from well 1 and the weak emission from well 2 are due to a lack of holes, i.e., holes are almost solely confined to well 3. Again, in the PL spectra (not shown), emission from all three wells is visible if the excitation power is sufficiently high. At low excitation power, only well 1 is visible, even though this well is furthest away from the excitation source. Both the EL data and the PL data agree with the assumption that there is in this structure significant electron transport between the different wells, and that this transport is directed toward the deepest well (in this case well 3).

Sample C is similar to sample B, except that the wells are thicker. The EL spectral peak is at a longer wavelength (550 nm) and a blueshifting and broadening of the peak with

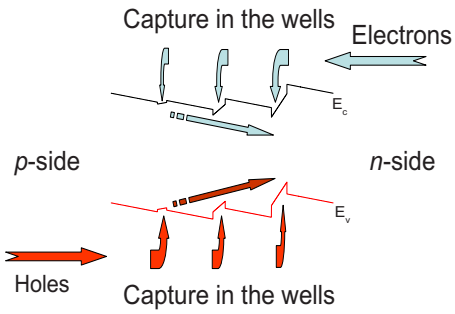

FIG. 5. (Color online) Schematic showing carrier capture and the transport of both electrons and holes toward the deeper quantum wells for sample A. The band diagram was calculated using BandEng.

increasing bias are evident. As in sample B, the deepest well (well 3) dominates. The difference is that there is now a more pronounced contribution from well 2. We suggest that the cause for this is a longer radiative recombination lifetime in the thicker quantum well (in the presence of a strong piezoelectric effect). As a result the holes have more time to escape into well 2 where they recombine radiatively with higher efficiency. The super linear *L-I* characteristic is the result of the filling of the bands, the screening of the piezoelectric field, and also an improved overlap of the electron and hole concentrations across the MQW region, as the bias levels increase.

Sample D is similar to sample A, except that the wells are thicker. In sample D we measure a dominant emission from the central well. The emission from the deepest well, which in sample A was competing with the central well, has almost disappeared. This is again attributed to a reduced carrier transport between the thicker quantum wells, allowing fewer holes to reach well 1. The fact that emission from well 1 is very weak on sample D means that very few holes reach this well, i.e., almost all holes are captured in wells 3 and 2. Similarly, the fact that the emission from well 3 is very weak means that very few electrons are captured directly into well 3, i.e., almost all electrons are captured in wells 1 and 2.

In summary, by analyzing the EL spectra from different MQW structures, we have shown that there is significant transport of captured carriers between the different quantum wells and that the net flow of these carriers is toward the deepest quantum well. We also noted that the voltage at low currents corresponds to the color of the dominating well.

We acknowledge financial support from Enterprise Ireland through Grant No. CFTD 06-304.

[1]Y. C. Shen, G. O. Mueller, S. Watanabe, N. F. Gardner, A. Munkholm, and M. R. Krames, Appl. Phys. Lett. **91**, 141101 (2007).
[2]N. F. Gardner, G. O. Muller, Y. C. Shen, G. Chen, S. Watanabe, and M. R. Krames, Appl. Phys. Lett. **91**, 243506 (2007).
[3]M. Peter, A. Laubsch, P. Stauss, A. Walter, J. Baur, and B. Hahn, Phys. Status Solidi C **5**, 2050 (2008).
[4]Y. L. Li, Th. Gessmann, and E. F. Schubert, J. Appl. Phys. **94**, 2167 (2003).
[5]J. P. Liu, J.-H. Ryou, R. D. Dupuis, J. Han, G. D. Shen, and H. B. Wang, Appl. Phys. Lett. **93**, 021102 (2008).
[6]S. W. Feng, C. C. Pan, J. I. Chyi, C. N. Kuo, and K. H. Chen, Phys. Status Solidi C **4**, 2716 (2007).
[7]Y. D. Qi, H. Liang, D. Wang, Z. D. Lu, W. Tang, and K. M. Lau, Appl. Phys. Lett. **86**, 101903 (2005).
[8]A. David, M. J. Grundmann, J. F. Kaeding, N. F. Gardner, T. G. Mihopoulos, and M. R. Krames, Appl. Phys. Lett. **92**, 053502 (2008).
[9]M. J. Hamp, D. T. Cassidy, B. J. Robinson, Q. C. Zhao, and D. A. Thompson, IEEE Photonics Technol. Lett. **12**, 134 (2000).
[10]T. Wang, J. Bai, and S. Sakai, Appl. Phys. Lett. **78**, 2617 (2001).
[11]A. Laubsch, M. Sabathil, G. Bruederl, J. Wagner, M. Strassburg, E. Baur, H. Braun, U. T. Schwarz, A. Lell, S. Lutgen, N. Linder, R. Oberschmid, and B. Hahn, Proc. SPIE **6486**, 64860J (2007).
[12]M. Grundmann, BANDENG, 2005, http://my.ece.ucsb.edu/mgrundmann/bandeng.htm.